DMD Fast Forward. Published on December 22, 2021 as DOI: 10.1124/dmd.121.000720
This article has not been copyedited and formatted. The final version may differ from this version.

Full paper:

Accelerating clinical development of idasanutlin through a physiologically-based pharmacokinetic modeling risk assessment for CYP450 isoenzyme related drug-drug interactions

Kenichi Umehara, Yumi Cleary, Stephen Fowler, Neil Parrott, Dietrich Tuerck

Roche Pharmaceutical Research and Early Development, Roche Innovation Center Basel, Grenzacherstrasse 124, CH-4070 Basel, Switzerland (K.U., Y.C., S.F., N.P., D.T.)

Running title: DDI-PBPK modeling of idasanutlin

Corresponding Author: Kenichi Umehara, Ph.D.

Roche Pharmaceutical Research and Early Development, Grenzacherstrasse 124, CH-4070 Basel, Switzerland.

Tel.: +41-61-68-80821

E-mail: kenichi.umehara@roche.com

Text pages:	35
Tables:	5
Figures:	5
References:	32
Abstract:	249 words (≤ 250)
Introduction:	701 words (≤ 750)
Discussion:	1,430 words (≤ 1,500)
Supplementary Document:	2
Supplementary Tables:	4
Supplementary Figure:	5

Abbreviations: BCRP, Breast Cancer Resistance Protein; CV, coefficient of variation; DDI, drug-drug interaction; EC_{50}, concentration resulting in half-maximal induction; E_{max} (Ind_{max}), the maximal fold-induction; Fa, the fraction absorbed after oral dosing; Fg, the fraction available after intestinal metabolism; Fh, the fraction available after hepatic metabolism; fm, the fraction metabolized by the enzyme; ft, the fraction transported; fu(mic), unbound fraction in human liver microsomes; fu(gut), unbound

fraction in enterocytes; fu, unbound fraction in plasma; HLM, human liver microsomes; HSA, human serum albumin; AGP, α-glycoprotein; ka, oral absorption rate constant; kdeg, the apparent first-order degradation rate constant of the affected enzyme; Ki, inhibition constant; Kp, tissue-to-plasma concentration ratio; MBP, microprecipitated bulk powder; MDR, multidrug resistance; MW, molecular weight; NTCP, Na-taurocholate co-transporting polypeptide; OATP, Organic Anion Transporting Polypeptide; PBPK, physiologically-based pharmacokinetic; PK, pharmacokinetics; P Caco-2, Caco-2 permeability; Peff,man, in vivo human intestinal effective permeability; P-gp, P-glycoprotein; Qgut, nominal flow in gut; r/r AML, relapsed/refractory Acute Myeloid Leukemia; Rb, blood-to-plasma concentration ratio; SDP, Spray-dried powder SDP; Vss, volume of distribution at steady-state

Abstract

Idasanutlin is a potent inhibitor of the p53-MDM2 interaction that enables re-activation of the p53 pathway which induces cell cycle arrest and/or apoptosis in tumor cells expressing functional p53. It was investigated for the treatment of solid tumors and several hematological indications such as relapsed/refractory acute myeloid leukemia, polycythemia vera or non-hodgkin lymphoma. For safety reasons it cannot be given in healthy volunteers for drug-drug interaction (DDI) explorations. This triggered the need for in silico explorations on top of the one available CYP3A clinical DDI study with posaconazole in solid tumor patients. Idasanutlin's clearance is dependent on CYP3A4/2C8, forming its major circulating metabolite M4, with contributions from UGT1A3 and biliary excretion. Idasanutlin and M4 have low permeability, very low clearance and extremely low unbound fraction in plasma (<0.001) which makes in vitro data showing inhibition on CYP3A4/2C8 enzymes challenging to translate to clinical relevance. PBPK models of idasanutlin and M4 have been established to simulate perpetrator and victim DDI scenarios and to evaluate whether further DDI studies in oncology patients are necessary. Modelling indicated that idasanutlin and M4 would show no or weak clinical inhibition of selective CYP3A4/2C8 substrates. Co-administered strong CYP3A and CYP2C8 inhibitors might lead to weak or moderate idasanutlin exposure increases and the strong inducer rifampicin might cause moderate exposure reduction. Since the simulated idasanutlin systemic exposure changes would be within the range of observed intrinsic variability, the target population can take co-medications which are either CYP2C8/3A4 inhibitors or weak/moderate CYP2C8/3A4 inducers without dose adjustment.

DMD Fast Forward. Published on December 22, 2021 as DOI: 10.1124/dmd.121.000720
This article has not been copyedited and formatted. The final version may differ from this version.

Significant Statement

Clinical trials for idasanutlin are restricted to cancer patients, which imposes practical, scientific and ethical challenges on DDI investigations. Furthermore, idasanutlin and its major circulating metabolite have very challenging ADME profiles including high protein binding, low permeability and a combination of different elimination pathways each with extremely low clearance. Nonetheless, PBPK models could be established and applied for DDI risk assessment and were especially useful to provide guidance on concomitant medications in patients.

Introduction

Cancer remains a major cause of morbidity and mortality worldwide despite recent progress with drugs providing survival benefit to patients. TP53 is a tumor suppressor gene, which is frequently mutated or deleted in human cancers, leading to a dysfunctional p53 tumor suppressor protein and facilitating uncontrolled cell proliferation (Chene 2003). In addition, p53 can be inactivated through protein degradation, which is triggered by binding to the E3 ligase MDM2, the main negative regulator of p53 (Moll et al., 2003, Kubbutat et al., 1997, Haupt et al., 1997). Therefore, in cancers with wild-type TP53 (TP53-WT), which includes a large proportion of patients with acute myeloid leukemia AML (≈80%) (Melo et al., 2002, Kadia et al., 2016, Yee et al., 2021), targeting MDM2 may be a promising therapeutic strategy to stabilize p53 levels and activate p53 tumor suppressor function and downstream apoptotic pathways.

Idasanutlin is a novel, potent and selective small-molecule MDM2 antagonist (Ding et al., 2013). Preclinical evaluations showed anti-tumor activity of idasanutlin in various indications (Higgins et al., 2013, Herting et al., 2018). In the clinic idasanutlin was investigated for acute myeloid leukemia as primary indication (Yee et al., 2021), solid tumors (Italiano et al. 2021), polycythemia vera (Mascarenhas et al., 2019) and nonhodgkin lymphoma were explored as well.

Common to all indications is the fragile nature of the patients. This makes it ethically questionable to perform a series of exploratory drug-drug interaction (DDI) studies in patients and idasanutlin cannot be given to healthy volunteers for this purpose due to cytotoxicity. The low incidence of the mainly explored relapsed/refractory acute myeloid leukemia (r/r AML) indication and the short life expectancy of these patients would also lead to a much extended clinical DDI program.

In vitro studies in human liver microsomes (HLM) with idasanutlin and its major circulating metabolite M4 showed reversible inhibition of CYP2C8 (0.164 μM, 0.13 μM) and CYP3A4 (>50 μM, 9.2 μM), respectively. The static mechanistic model calculation for idasanutlin using the CYP inhibition study data in human liver microsomes (HLM) leads to predictions of AUC increases for probe substrates of CYP2C8 (paclitaxel, fm = 0.87 and F_g =1) and CYP3A4 (midazolam, fm = 0.95 and F_g = 0.51) (Njuguna et al., 2016) of 3.54-fold and 1.49-fold, respectively, with multiple oral administrations of idasanutlin at a therapeutic oral dose of 300 mg (Supplementary Table S1). Similarly, static model assessment for its major circulating metabolite M4 alone, predicts an AUC increase of 1.58-fold for paclitaxel due to inhibited CYP2C8 metabolism (Supplementary Table S1). Free fractions in plasma were not measurable (≤0.001 for both molecules) and so, according to the static mechanistic model (FDA, 2020), an unbound fraction (f_u) of 0.01 has to be assumed, resulting in exaggerated predictions of the inhibition DDI risk.

Idasanutlin might also possess a victim DDI liability since systemic exposure changes are expected when dosed with co-medications which are perpetrators of CYP3A4 and/or CYP2C8. Based on the in vitro, pre-clinical and human mass balance study results, idasanutlin was mainly metabolized by CYP3A4, CYP2C8 and UGT1A3, with some direct biliary excretion also contributing to total clearance (Papai et al., 2019, Glenn et al., 2016). Elimination pathways of M4 were postulated based on the human mass balance study of idasanutlin and included oxidative metabolism, as well as contributions of efflux transporters and direct glucuronidation. The fractional contributions of the various metabolic pathways to hepatic elimination of idasanutlin and M4 could not be fully estimated in vitro due to the extremely low hepatic intrinsic clearance values. Therefore, the clinical impact of posaconazole on the PK of

idasanutlin provided useful insight into the in vivo fraction metabolized by CYP3A4 (fm,CYP3A4), which was still unclear from the in vitro data.

A comprehensive physiologically-based pharmacokinetic (PBPK) model of idasanutlin and its metabolite M4 was developed to combine all available data and obtain a more realistic risk estimate than was provided by the static model. It provides a risk assessment with respect to CYP enzyme (2C8 and 3A4) inhibition with idasanutlin as perpetrator and victim. Inhibitory effects of idasanutlin/M4 on the PK of CYP3A4 and CYP2C8 standard substrates (i.e. midazolam, repaglinide) were evaluated and the systemic exposure changes of idasanutlin in the presence of CYP3A4/CYP2C8 inhibitors and inducers were simulated (Table 1).

Materials and Methods

Input parameters in the PBPK model of idasanutlin and metabolite M4. All simulations were performed using SimCYP Simulator (Version 18; Certara Inc., Princeton, NJ). The input parameters for the models of idasanutlin and its major metabolite M4 with derivations are summarized in Table 2. The drug disposition pathways and the model building process are illustrated in Figure 1 and Figure 2, respectively. The quantitative contributions of the disposition pathways of metabolite M4 could not be investigated for technical reasons e.g. extremely low turnover in vitro, therefore, the current PBPK model of this metabolite was used for DDI risk assessment as a perpetrator, but not as a victim. This is in alignment with expectations set out in the FDA DDI guidance document (2020). Metabolite M4 contributes only minimally to the pharmacological activity of idasanutlin (about 20 % of the parents activity in vitro [data not shown] combined with lower exposure as the parent), and the systemic exposure of M4 is <20% relative to the parent drug idasanutlin and M4 was not further metabolized to major circulating or pharmacologically relevant metabolites (Figure 3, Supplementary Table S4). A population file of healthy volunteers in SimCYP was used for all simulations conducted in this study, due to a lack of information of the impact of the target disease status on patient physiology. Age, body height and weight distribution of the virtual population were adjusted to match the respective study patient population.

Absorption. The permeability of idasanutlin in Caco-2 cells was low in the apical to basal direction (0.8×10^{-6} cm/s). The intestinal absorption of idasanutlin was likely governed by passive permeation, consistent with a T_{max} after oral doses of several hours. Idasanutlin is not a substrate of P-gp or BCRP. This is supported by efflux ratios of 1.0 and 0.6 in MDCK II-MDR1 cells (cells obtained from Prof. Yuichi Sugiyama,

Tokyo, Japan) in two independent experiments, suggesting no directional transport (5 μM). In addition, uptake of idasanutlin (2 μM) by membrane vesicles prepared from human BCRP-expressing insect cells (SOLVO Biotechnology; Szeged, Hungary) was not ATP-dependent and was not inhibited by the control inhibitor Ko143 (1 μM), indicating mostly unspecific binding. Therefore, an empirical 1st order absorption model was applied with the fraction absorbed (F_a) based on the clinically determined oral absolute bioavailability (F) in the fed state of 0.4 and 0.187 for a spray-dried powder (SDP) and microprecipitated bulk powder (MBP) formulation of idasanutlin respectively. The approximation of F_a = F was considered to be reasonable since the fractions escaping metabolism in intestine and liver (F_gF_h) after oral administration were estimated to be ≥0.99 based on clinical pharmacokinetics measured after intravenous dosing and a DDI study in the absence and presence of posaconazole (discussed below). Idasanutlin was metabolized by CYP3A4 and CYP2C8 with low intrinsic clearance, and the contribution of CYP3A4 to total elimination was low. The SDP formulation has been used in the most recent clinical studies, and so to simulate a worst case for the DDI risk assessment of idasanutlin as a perpetrator, a high F_a (0.4) was used as model input. A first order oral absorption rate constant (k_a) was estimated using the mechanistic absorption model (SimCYP Version 18) using the permeability of idasanutlin in Caco-2 cells in the apical to basolateral direction (0.8×10^{-6} cm/s), which captured the PK profiles well based on visual inspection (Figure 3). Modification of ka did not affect the DDI prediction results (Supplementary Figures S1, S2, S3 and S4).

An unbound fraction in enterocyte $f_{u(gut)}$ for idasanutlin was set to 0.001 for idasanutlin. For the metabolite M4 a value of 1 was assumed in order to maximize the potential clinical DDI prediction even though M4 shows relatively low systemic

exposure compared to the parent drug idasanutlin. This assumption was further explored by running sensitivity analysis to investigate the impact of changing $f_{u(gut)}$ on DDI potential (Supplementary Figures S3 and S4).

Distribution. The volume of distribution of idasanutlin at steady state V_{ss} (0.40 L/kg) was initially predicted using the tissue to plasma partition coefficient (K_p) values determined in a quantitative whole body autography study in rats, and then by scaling of all the K_p values by 50% to achieve V_{ss} and plasma concentration–time profiles consistent with the pharmacokinetics in human after intravenous (i.v.) administration of [^{13}C]idasanutlin. Given the similar physicochemical properties of idasanutlin and its metabolite M4, an identical K_p adjustment was applied for the PBPK model of the metabolite.

Definitive unbound fractions in plasma (f_u) for idasanutlin and metabolite M4 could not be measured due to the extremely low values of < 0.001. To simulate a worst case scenario for the CYP inhibitory potential, the highest possible f_u of 0.001 was implemented for both compounds. The blood-to-plasma concentration ratio of idasanutlin was measured as 0.64.

Metabolism. A fm,CYP3A4 was estimated using data from a clinical DDI study with posaconazole (Nemunaitis, et al., 2018). Two-dimensional analysis (Cleary et al. 2018) simultaneously estimated fm,CYP3A4 and F_g from the fold-change in C_{max} and AUC of idasanutlin after co-administration of posaconazole. The estimated in vivo fm,CYP3A4 and F_g of idasanutlin were 0.25 and 0.99, respectively (Supplementary Figure S5).

Based on the in vitro enzymology study results using recombinant enzymes, idasanutlin was mainly metabolized by CYP3A4, CYP2C8 and UGT1A3. The oxidative metabolism of idasanutlin at 1 μM using HLM supplemented with NADPH was inhibited

by approximately 50% and 50% in the presence of 3 µM montelukast (CYP2C8 inhibitor) and 1 µM ketoconazole (CYP3A4 inhibitor), respectively. Since unbound idasanutlin concentration after clinically relevant doses was < 1 µM, equal contribution of CYP2C8 and CYP3A was expected. Hence, fractions metabolized by CYP2C8 and CYP3A4 compared to total clearance were both estimated to be 0.25 and the remaining fraction of 0.5 was assigned to the other elimination pathways of UGT1A3 metabolism and biliary excretion. The intrinsic clearance values due to human CYP2C8 and CYP3A4 enzymes were back-calculated using the well-stirred liver model by considering the fractional contributions to total clearance, enzyme abundances and other physiological data. An additional intrinsic clearance in HLM was added to the model to represent the sum of the other elimination pathways. It was not possible to calculate separately the fractions of UGT1A3 and biliary excretion for idasanutlin as the glucuronide was not recovered in human feces.

Hepatic intrinsic clearance of idasanutlin (based on unbound concentration) was back-calculated to be 220 µL/min/mg protein corresponding to 8.76 mL/min/g liver using a microsomal protein content in liver (38 mg/g liver; SimCYP Version 18). The combination of intrinsic clearance by CYP3A4/2C8 as well as UGT1A3 with potential biliary excretion would therefore be 110 µL/min/mg protein in each, since, as stated above, an equal contribution of CYPs (CYP3A4 and CYP2C8) and the other pathways (UGT1A3 and biliary excretion) was expected.

Elimination. There was no relevant urinary excretion of idasanutlin in the human mass balance study with <0.1% of the radioactive dose recovered in the urine (Papai et al., 2019). In feces, unchanged idasanutlin was the major drug component accounting for 84.2% of the dose in the pooled feces samples between 0 and 264 h after oral administration of [^{14}C]-idasanutlin.

CYP3A4 and CYP2C8 catalyzed the formation of M2 from idasanutlin and M2 was further metabolized to M4 based on the data from incubation with recombinant enzymes and human preparations. Therefore, the assigned intrinsic clearance of idasanutlin due to CYP3A4 and CYP2C8 was regarded as being the same as the M4 "formation clearance" with the hepatic intrinsic clearance of 110 µL/min/mg protein corresponding to 4.38 mL/min/g liver stated as above. Due to the extremely low turnover the total elimination clearance of metabolite M4 [1.76 L/h corresponding to 0.02 mL/min/g liver using 22 g liver/kg bw (Johnson et al., 2005) and a body weight of 80 kg] in the model was adapted to capture the observed plasma concentration profiles over time after the last dose of idasanutlin based on visual inspections (Yee et al., 2021). Along the same line, the fractions of the disposition pathways relative to total elimination of the metabolite have not been investigated. The elimination pathways of the metabolite M4 were postulated based on the human mass balance study of idasanutlin and included oxidative metabolism, passive or active efflux (3.4% of the idasanutlin dose accounted for metabolite M4 in feces) and direct glucuronidation (traces in human plasma).

Impact of transport on hepatic drug disposition. Idasanutlin and metabolite M4 were not substrates of the active uptake transporters OATP1B1 and OATP1B3.

Although a potential contribution of biliary excretion to hepatic clearance of idasanutlin was indicated, idasanutlin was not a substrate of the efflux transporters P-gp and BCRP. Less involvement of biliary excretion of the metabolite M4 in total clearance was indicated by the human mass balance study results.

CYP DDI inputs with idasanutlin as perpetrator. In vitro studies with idasanutlin in HLM showed reversible inhibition of CYP1A2, CYP2B6, CYP2C8, CYP2C9, CYP2C19, CYP2D6, CYP3A4 and CYP2E1 (no time-dependent inhibition (TDI)).

According to the net effect model (FDA, 2020), assuming an unbound fraction in plasma f_u of 0.01, AUC increases were calculated for probe substrates for CYP2C8 (paclitaxel) and CYP3A4 (midazolam) after multiple oral administration of idasanutlin at a therapeutic oral dose 300 mg - and were 3.54-fold for CYP2C8 and 1.49-fold for CYP3A4, respectively (Supplementary Table S1). There was no induction effect on mRNA levels of CYP1A2, CYP2B6 and CYP3A4 after 24-72 h exposure of idasanutlin (up to 3 µM) to hepatocytes from five individual liver donors and therefore induction effects were not considered further.

CYP DDI inputs with metabolite M4 as perpetrator. In vitro studies with the major circulating metabolite M4 in HLM showed reversible inhibition of CYP1A2, CYP2B6, CYP2C8, CYP2C9, CYP2C19, CYP2D6 and CYP3A4 (no TDI). The net effect model assessment for the circulating metabolite M4 estimated an AUC ratio of 1.58 due to inhibition of paclitaxel CYP2C8 metabolism if using a f_u of 0.01 (as the unlikely worst case scenario; Supplementary Table S1). Induction effects of metabolite M4 on mRNA and enzyme activity level of CYP1A2, CYP2B6 and CYP3A4 were not observed for metabolite M4 after 24-72 h exposure of the metabolite (up to 10 µM) to hepatocytes from five individual liver donors.

Simulation of PK profiles after multiple oral administration of idasanutlin using established PBPK models. PK parameters of idasanutlin and metabolite M4 were simulated after a single intravenous idasanutlin dose (0.1 mg), and after multiple oral administrations of idasanutlin 400 mg at day 1, 10 and 19. The 400 mg dose was originally planned but later, dosing was changed to 300 mg given on 5 consecutive days at the start of a 28 day treatment cycle. The PK data from (Yee et al, 2021) were used as reference data to assess the predictability of PK profiles using the PBPK models of the two compounds (Supplementary Table S2).

CYP DDI risks via idasanutlin and metabolite M4 as perpetrator with PBPK modeling. Simulations were performed to investigate the DDI due to multiple idasanutlin doses (300 mg twice daily for 5 days) on single oral administrations of midazolam (2 mg) and repaglinide (0.25 mg) (Supplementary Table S2).

PBPK modeling of idasanutlin as a victim of CYP inhibition. The predicted changes of systemic exposures of idasanutlin (800 mg p.o., single dose) following multiple oral administration of posaconazole (at 400 mg twice daily) could be compared to the actually obtained clinical DDI data (Nemunaitis, et al., 2018). The DDI risks of idasanutlin as victim were assessed in single (300 mg p.o. at day 5, 7 or 15) and multiple administration schedules (300 mg twice daily). Assessments were made for the following orally administered perpetrators: 1) strong CYP3A4 inhibitors (ketoconazole: 200 mg twice daily and itraconazole: 200 mg once daily), 2) moderate CYP3A4 inhibitors (erythromycin: 500 mg twice daily and fluconazole: 200 mg once daily), 3) weak CYP3A4 inhibitor (fluvoxamine: 50 mg, once daily), 4) CYP2C8 inhibitor (gemfibrozil: 600 mg twice daily) and/or 5) CYP3A4(/2C8) inducers (efavirenz: 600 mg and rifampicin: 600 mg once daily) (Supplementary Table S2; results in Figure 5 for single idasanutlin doses).

Explored PBPK models of CYP perpetrators (idasanutlin as victim). SimCYP Version 18 library models of the CYP3A4 and 2C8 perpetrators [ketoconazole, itraconazole including its hydroxyl metabolite (capsule formulation; at fed state), erythromycin, fluconazole, fluvoxamine, efavirenz, gemfibrozil including gemfibrozil 1-O-β-glucuronide] were used with their respective model verification documents. Input parameters and model verification/performance for the posaconazole model as a strong CYP3A4 inhibitor have been published elsewhere (Cleary et al., 2018).

Rifampicin is classified as a strong CYP3A4 and CYP2C8 inducer in vivo (FDA, 2020). The compound file for rifampicin in SimCYP Version 13 was updated for predictions of CYP3A4 induction potential by transferring input parameters from a published rifampicin model (Baneyx et al., 2014). The model incorporated enzyme kinetic data for rifampicin metabolism by CYP3A4, which resulted in successful prediction of the slight auto-induction of CYP3A4 with reduction of the systemic exposures of rifampicin after multiple oral administrations. The updated rifampicin model could reasonably capture the induction effects on the PK of CYP3A4 substrates. In addition, the maximum fold-induction Ind_{max} ($=E_{max}+1$) for CYP2C8 by rifampicin was adjusted to match observed systemic exposure reductions for rosiglitazone (8 mg p.o., single dose at day 6) after co-administration of rifampicin 600 mg, once daily for 6 days (Park et al., 2004). The concentrations needed to trigger half-maximal induction (EC_{50}) for CYP2C8 and for CYP3A4 were assumed to be identical, since the induction mechanism for both enzymes involves activation of the same nuclear receptor (pregnane X receptor; PXR). Rosiglitazone is metabolized by CYP2C8, CYP2C9 and additional unidentified hepatic metabolism with respective fm values of 0.58, 0.29 and 0.13 (SimCYP model verification document). For the rifampicin CYP2C8 Ind_{max} adjustment, it was assumed that the unidentified metabolism pathways of rosiglitazone are not induced on co-medication of rifampicin. The rifampicin model might, therefore, overestimate the induction potential of rifampicin on CYP2C8 which is in line with the objective to investigate a worst case scenario for the DDI potential with idasanutlin as victim.

Input parameters and model verification/performance for the rifampicin model as a CYP3A4 and CYP2C8 inducer were summarized in Supplementary Table S3 and Information S1, respectively.

PBPK models of standard victim drugs with idasanutlin as perpetrator. Verified SimCYP Version 18 library models of midazolam (CYP3A4 substrate), repaglinide (CYP2C8 substrate) and rosiglitazone (CYP2C8 substrate) were used for this purpose.

Qualification of PBPK modeling software. With respect to qualification of PBPK for DDI risk assessment, SimCYP DDI predictions of CYP3A4 reversible and time-dependent inhibition have been reported for 30 drugs, showing a good predictability for clinical DDIs with midazolam (Fahmi et al., 2009). In addition, 20 clinical DDI study results showed greater than 20% decreases in the exposure of CYP3A4 substrates were predicted using SimCYP (Bolleddula et al, 2021) in the presence of the moderate and strong inducers. Based on these qualifications, the PBPK platform SimCYP is considered to provide useful DDI risk assessments for reversible and time-dependent inhibition, as well as for induction of CYP3A4. The systemic exposure increases of the dual substrates of CYP3A4 and CYP2C8 repaglinide and rosiglitazone after co-administration of an inhibitor of CYP2C8 (gemfibrozil) were successfully predicted as reported in the SimCYP model verification documents. Given that PBPK models for CYP3A4 substrates have been qualified, the PBPK platform SimCYP can also be used for DDI risk assessments due to inhibition of CYP2C8. Due to the lack of clinical reference data showing induction effects on CYP2C8, it is difficult to demonstrate a qualification of the SimCYP software for predictions of CYP2C8 induction. However, the performance of a newly modified rifampicin file as a CYP2C8 inducer was provided in Supplementary Information S1. The predicted AUC ratio of rosiglitazone at 8 mg (single dose, p.o.) with co-medication of rifampicin (600 mg, once daily) was 0.30, which is reasonably comparable to the observation (0.34).

Simulation design parameters for PBPK modeling. The simulation trial design parameter including demographic parameters were taken directly from the actual treatment cycle of this drug; otherwise, generic designs were applied as provided in Supplementary Table S2. For the current simulation work, an idasanutlin dose of 400 mg was taken, which was the originally planned clinical dose, later reduced to 300 mg dose in adults and presents now a worst case scenario.

Data representation for simulated DDI scenarios. All the systemic pharmacokinetic data were based on plasma concentrations. The predicted AUC, C_{max} and T_{max} for idasanutlin and its metabolite M4 are shown as geometric means or medians with coefficient of variation CV(%) or range. The exposure change in the presence of perpetrators was presented as AUC ratio and/or C_{max} ratio. The predictability of PK parameters and AUC/C_{max} ratios due to CYP3A4 DDI was evaluated using the criteria of geometric means within 2-fold errors (Fahmi et al., 2008).

Clinical pharmacology studies included in the PBPK modelling. A mass balance study including an intravenous microdose, a posaconazole DDI study, a bioequivalence study and sparse data from a clinical efficacy study were available for the model development. The mass-balance of idasanutlin was investigated in eight patients who had a histologically or cytologically confirmed advanced malignancy (ClinicalTrials.gov Identifier: NCT02828930). The detail of the study is published elsewhere (Papai et al., 2019). In brief, the patients received 100 mg [^{14}C]-idasanutlin MBP and unlabelled 300 mg SDP formulations orally. Six hours after the oral administration, *i.e.* at around oral peak time, [^{13}C]-idasanutlin 100 μg was given intravenously to evaluate an absolute oral bioavailability of idasanutlin. Plasma, whole blood, urine and feces were collected up to 264h after idasanutlin administration.

The posaconazole DDI study explored the effect of concomitant administration of posaconazole, a potent CYP3A inhibitor, on idasanutlin PK in 18 patients [ClinicalTrials.gov Identifier: NCT01901172 (Nemunaitis, et al., 2018)]. Posaconazole 400 mg was given twice a daily for 7 days, and 800 mg idasanutlin as MBP formulation was given as a single dose 4 days after the initiation of posaconazole treatment. Plasma samples were collected to quantify idasanutlin and metabolite M4 up to 264 h after oral administration of idasanutlin. A bioequivalence in solid tumor patients investigated single doses of three SDP tablet formulations at a dose level of 300 mg (ClinicalTrials.gov Identifier: NCT03362723).

Safety, PK and preliminary efficacy of idasanutlin was investigated in 122 patients with AML [ClinicalTrials.gov Identifier: NCT01773408 (Yee et al, 2021)]. The patients received 400-1600 mg of MBP formulation or 600-800 mg/day of SDP formulations (300 or 400 mg twice a daily) for 5 days followed by 23 days with no idasanutlin administration. Plasma samples were collected from these participating patients across available cycles to quantify idasanutlin and metabolite M4 concentrations.

All relevant study documents of the clinical studies were approved by the Institutional Review Board and all subjects signed the informed consent forms prior to enrollment. These studies were conducted in full conformance with the principles of the Declaration of Helsinki. Plasma concentration of idasanutlin, M4 and [^{13}C]-idasanutlin were measured by specific liquid chromatography–tandem mass spectrometry methods.

DMD Fast Forward. Published on December 22, 2021 as DOI: 10.1124/dmd.121.000720
This article has not been copyedited and formatted. The final version may differ from this version.

Results

PK predictions of idasanutlin and metabolite M4. The PBPK model predictions were in a good agreement with the observed concentration-time profiles. The mean AUC_{inf} after single intravenous administration of idasanutlin at 0.1 mg (n = 80) was estimated to be 156 ng·h/mL, which is very comparable with the actually observed 150 ng·h/mL (n = 8; Supplementary Table S4). Predicted $AUC_{(0-t)}$, C_{max} and T_{max} of idasanutlin in plasma after oral administration of 400 mg idasanutlin were 225000 ng·h/mL, 4300 ng/mL, and 7.8 h, respectively. The estimated $AUC_{(0-t)}$, C_{max} and T_{max} values of the metabolite M4 for the simulated idasanutlin dose regimen were 46800 ng·h/mL, 601 ng/mL and 28 h, respectively (Supplementary Table S4).

Over all, the predicted plasma $AUC_{(0-t)}$ and C_{max} were in line with the observations in the bioequivalence study due to the intra-individual variability (coefficient of variation of 25-30%) (Supplementary Table S4).

CYP DDI simulations with idasanutlin and metabolite M4 as perpetrator with respect to CYP3A4 and CYP2C8. The idasanutlin PBPK model including metabolite M4 predicted no relevant change of the AUC ratio (1.20) and C_{max} ratio (1.19) for the CY3A4 substrate midazolam (2 mg p.o., single dose on day 5) after repeated co-administration of idasanutlin with 300 mg p.o., twice daily (Table 3). As the idasanutlin PBPK model without inclusion of metabolite M4 simulated no systemic exposure increase of midazolam, the metabolite M4 did not alter the in vivo inhibition potential prediction on CYP3A4.

Repaglinide was used as a victim for CYP2C8, although it is also a substrate of OATP1B1 and CYP3A4 (Table 1). However, the exploration above showed that idasanutlin or metabolite M4 have no relevant effect on CYP3A4, which is also true for OATP1B1 according to in vitro data (in house data). Repaglinide can, therefore, be

used as the probe CYP2C8 substrate in this study. The PBPK model for idasanutlin including metabolite M4 predicted geometric mean ratio changes of 1.96 and 1.48 for AUC and C_{max} for repaglinide, respectively (0.25 mg repaglinide after repeated idasanutlin doses of 300 mg p.o., twice daily), indicating no relevant interaction (Table 3). A slightly lower systemic exposure change of repaglinide was simulated without metabolite M4 (AUC ratio 1.61 instead of 1.96). Therefore it is clear that the parent drug dominates the net perpetrator DDI potential towards CYP2C8.

Idasanutlin DDI as a victim of CYP3A4 and CYP2C8 inhibition. Idasanutlin C_{max} and AUC_{inf} changed following oral administration of a strong CYP3A4 inhibitor (posaconazole 400 mg twice daily) by a factor of 0.94 and 1.31, respectively (Table 4). Based on these limited changes, a two-dimensional analysis was performed (Cleary et al. 2018) to estimate simultaneously the in vivo idasanutlin fm,CYP3A4 and F_g and yielded values of 0.25 and 0.99, respectively (Supplementary Figure S5). Implementation of these fm,CYP3A4 and F_g values into the idasanutlin PBPK model adequately recovered observed PK parameters (Table 4) and plasma concentration-time profiles (Figure 4) of idasanutlin in the presence of posaconazole. The effect of concomitant medications with various magnitude of CYP3A4/2C8 inhibition and induction on the systemic exposure of idasanutlin (300 mg p.o.; single dose) was summarized in Figure 5 and Supplementary information S2.

As idasanutlin was given at 300 mg p.o. (twice daily) for five days in 28 day cycles (Yee et al., 2021), the DDI prediction with idasanutlin as victim after multiple dosing was clinically relevant and of interest for drug development. The predicted AUC and C_{max} ratios of idasanutlin with co-medication of itraconazole (200 mg p.o., once daily for 30 days) were 1.21 (range: 1.08-1.42) and 1.17 (range: 1.07-1.33) - as well as 1.24 (range: 1.03-2.11) and 1.22 (range: 1.02-2.00) for the co-administration of

gemfibrozil (600 mg p.o., twice daily for 15 days), respectively. The ratios after simultaneous co-administration of gemfibrozil (600 mg p.o., twice daily) and ketoconazole (200 mg p.o., twice daily) were predicted to be 1.60 (range: 1.11-2.63) for AUC and 1.57 (range: 1.11-2.43) for C_{max}. The changes in the presence of rifampicin (600 mg p.o., once daily for 15 days) were 0.24 (range: 0.15-0.45) for AUC and 0.35 (range: 0.25-0.50) for C_{max}, respectively (Table 5).

The numerically slightly different AUC and Cmax changes after single and repeated idasanutlin doses can be seen in the forest plot (Figure 5) and Supplementary Tables IIA and IIB.

Discussion

The objective of the current study was to provide a DDI risk assessment for idasanutlin based on limited clinical data by means of in vitro and in silico approaches. Clinical Phase 1 studies were available to develop a PBPK model and to validate the predictions using the available CYP3A inhibition study with posaconazole as perpetrator. The obtained results were then applied to predict the outcome of further DDI studies with idasanutlin as victim and perpetrator, with respect to CYP3A4 and CYP2C8. This could support the use of co-medications with idasanutlin. Limiting factors were 1) the extremely high protein binding with no measurable free fractions (i.e. <0.1%), and 2) the very limited possibility to perform clinical drug-drug interaction studies.

Clinically relevant idasanutlin exposure increases are not expected on co-dosing of strong CYP3A4 or CYP2C8 inhibitors (predicted geometric mean AUC increase: 1.21-fold and 1.24-fold for itraconazole and gemfibrozil co-administration, respectively), even if inhibitors for both enzymes are combined (1.60-fold for combined gemfibrozil and ketoconazole administration) (Table 5). This outcome was validated for CYP3A4 by the result of the available posaconazole interaction study, which showed an increase of only 31% AUC of idasanutlin AUC (Nemunaitis et al. 2017). In contrast to CYP inhibitors, CYP inducers may have relevant effects on idasanutlin's exposure. Rifampicin as a strong inducer may result in a relevant decrease in idasanutlin's exposure, with moderate (≥50% reduction in AUC) to strong (≥80%) AUC reductions (Table 5, Figure 5).

Perpetrator DDI simulations were performed to explore the effect of idasanutlin on the PK of midazolam (2 mg p.o., single dose) and repaglinide (0.25 mg p.o., single dose) (Table 3). It could be shown that idasanutlin may have no relevant effect on

CYP3A substrate exposure (geometric mean AUC increase 1.20-fold for midazolam). Only a weak effect is predicted for CYP2C8 substrates such as repaglinide (geometric mean AUC increase of 1.96-fold), although the CYP2C8 inhibition via idasanutlin or metabolite M4 was the strongest across all CYP isoenzymes. A higher impact on future drugs cleared solely by CYP2C8 cannot, however, be ruled out.

The validity of these DDI predictions are potentially challenged in the absence of further clinical studies, therefore several points might be considered: 1) The idasanutlin PBPK model for PK and DDI risk assessment adequately recovered the clinical data. PK data were available after intravenous (0.1 mg) and oral (400 mg) administrations (Supplementary Table S4), 2) The predicted effect of the strong CYP3A4 inhibitor posaconazole on the PK of idasanutlin using the PBPK model of idasanutlin with a fm,CYP3A4 of 0.25 was consistent with the observations (Table 4 and Figure 4), and 3) Furthermore, F_a and fecal excretion of the parent drug estimated in the human mass balance study could define the fractions excreted in bile and metabolized by UGT1A3 (Figure 1). The intestinal first pass effect via efflux transport and metabolism was likely to be negligible. While the F_g value based on the two-dimensional analysis was not used as an initial input parameter for the idasanutlin model (Supplementary Figure S5), the fm,CYP3A4 was aligned with the respective in vitro findings resulting in predicting a F_g of 1 with the back-calculated intrinsic clearance from the intravenous PK data. Across a panel of recombinant UGT enzymes, the contribution of UGT1A3 was shown to be predominant in forming the direct glucuronide in vitro. For the metabolite, the PBPK model used a total apparent clearance without specific enzyme assignment. The model has been established to predict AUC, C_{max} and T_{max} for metabolite M4 after repeated oral administration of idasanutlin in solid tumor cancer patients (Supplementary Table S4).

Considering prediction variability due to intra-individual differences in physiology and sensitive model parameters such as f_u and $f_{u(gut)}$, it should be considered that idasanutlin exposure itself showed an intra-individual coefficient of variation between 25% and 30% for idasanutlin alone, which puts smaller changes in idasanutlin exposure into perspective. The simulation results presented here, with inclusion of appropriate sensitivity analysis for uncertain model input parameters were important for the risk-benefit assessment of idasanutlin (Supplementary Figures S1, S2, S3 and S4), since conduct of further respective DDI studies was hardly feasible – or very time consuming if solid tumor patients would be considered instead of the r/r AML target population.

A few similar attempts to predict with PBPK modeling untested PK and DDI scenarios where running clinical studies is not feasible have been recently reported. Eliglustat was developed for Gaucher disease as a lysosomal storage disorder by a hereditary deficiency in the enzyme glucocerebrosidase. The PBPK model of this drug was used to qualify the impact of CYP2D6 polymorphisms and victim DDI risk assessment, and based on the prediction results FDA approved this drug for treatment of extensive, intermediate and poor metabolizers for CYP2D6 (Drugs@FDA, https://www.accessdata.fda.gov/drugsatfda_docs/nda/2014/205494Orig1s000ClinPharmR.pdf). Another example is venetoclax, *i.e.* a selective B-cell lymphoma-2 inhibitor that restores apoptosis in cancer cells, where a limited in vivo extrapolation with ketoconazole (CYP3A inhibition) and rifampicin (P-gp inhibition) was conducted, and further DDI studies were successfully waived for NDA submission with the aid of PBPK modeling (Freise et al., 2017; Emami Riedmaier et al., 2018).

Clinical DDI trials for idasanutlin could not be performed in healthy volunteers and restricted to cancer patients which imposes practical and ethical challenges for

clinical DDI investigations. Although the PBPK models were developed based on physiology of healthy volunteer virtual population with adaptation of the demographic model to the actual cancer patients, the model parameters were estimated and /or verified using idasanutlin PK (i.v. and p.o.), DDI and mass balance data collected from cancer patients. Therefore, potential effects of the disease status on predictions of idasanutlin's disposition and the DDI risk assessment have been captured in the current PBPK model.

Recently significantly lower expression of many CYPs and UGTs (likely except for UGT1A3, i.e. a metabolizing enzyme of idasanutlin) was reported using HLM prepared from colorectal cancer liver metastasis patients based on the proteomics approach (Vasilogianni et al., 2021). Several attempts to deploy PBPK modeling for disease-drug interactions have been made to describe the suppression effect of elevated levels of cytokines as IL-6 in patients relative to healthy volunteers on the activity of CYP enzymes. With the suppression kinetics of IL-6 on CYP1A2, 2C9, 2C19 and 3A4 in a concentration-dependent manner in vitro, the exposure of the in vivo CYP probe substrates as caffeine, S-warfarin, omeprazole, midazolam and simvastatin could be predicted as a function of the elevated levels of IL-6 (Xu et al., 2015; Jiang et al., 2016; Machavaram et al., 2019). Therefore, reduction of CYP3A4 abundance in the patients with the treatment of idasanutlin can be expected and this could imply the systemic exposure increase of idasanutlin and M4 due to CYP3A4-mediated CL reduction depending on the disease status. Nevertheless, these potential exposure differences may already have been accounted for to some extent due to the use of patient exposure data in model validation. Irrespective, no additive effects of the CYP3A4 down-regulation on the victim DDI magnitude of idasanutlin can be anticipated with a potentially lower fm,CYP3A4 relative to healthy volunteers. Along

the same line the perpetrator DDI risk on CYP3A4 can be further weak compared to the current simulation results due to the potential reduction of the CYP3A4 abundance.

Modification of plasma protein levels such as albumin in different hepatic and renal disease stages is also reported (Heimbach et al., 2021), which could potentially impact on the DDI risk assessment of idasanutlin showing an extremely high plasma protein binding. Interestingly, Crohns disease populations at an age range of 1-19 years old, a 2-fold reduction of villous length was observed in inflamed duodenum and ileum besides a decreased expression of CYP3A4 mRNA levels (Vyhlidal et al., 2021). This indicates the impact of disease status on F_a after oral absorption of a drug. Irrespectively, a changing F_a and f_u for idasanutlin and/or M4 was not sensitive to the perpetrator and victim DDI prediction results due to CYP3A4 (Supplementary Figures S1, S2, S3 and S4). Nonetheless, extrapolations of DDIs by modelling according to a translational strategy as such to overcome these difficulties together resulted in a meaningful characterization of DDI potential of the drug candidate for highly unmet medical needs, to support guidance for concomitant medications in patients.

As a consequence, it is predicted that the target patients could take co-medications of CYP2C8 and CYP3A4 inhibitors without any dose adjustment. On the contrary, the current recommendation to avoid concomitant use of rifampicin (or other strong inducers of CYP3A and CYP2C8) with idasanutlin was maintained. The target patients could still receive the benefit from taking idasanutlin with co-medication of other weak and moderate inducers of CYP2C8 and/or CYP3A4.

Acknowledgements

The authors wish to acknowledge Marie-Elise Brun and other scientists at F. Hoffmann-La Roche, Basel, who have supported generation of the data used in these analyses. Drs. Jianguo Zhi, Annie Young, Elena Guerini, Silke Simon, Susanne Mühlbauer and Christophe Schmitt for the discussion on clinical pharmacology study data.

Authorship Contributions

All five authors are employees of F. Hoffmann La Roche AG in Basel, Switzerland.

Participated in research designs: Umehara, Cleary, Fowler, Tuerck

Conducted experiments: Umehara, Cleary, Fowler

Performed data analysis: Umehara, Cleary, Fowler

Wrote or contributed to the writing of the manuscript: Umehara, Cleary, Fowler, Parrott, Tuerck

References

Baneyx G, Parrott N, Meille C, Iliadis A, and Lave T (2014) Physiologically based pharmacokinetic modeling of CYP3A4 induction by rifampicin in human: influence of time between substrate and inducer administration. *Eur J Pharm Sci* **56:**1-15.

Blotner, Steven, et al. "Phase 1 summary of plasma concentration–QTc analysis for idasanutlin, an MDM2 antagonist, in patients with advanced solid tumors and AML." *Cancer chemotherapy and pharmacology* 81.3 (2018): 597-607.

Bolleddula J, Ke A, Yang H, and Prakash C (2021) PBPK modeling to predict drug-drug interactions of ivosidenib as a perpetrator in cancer patients and qualification of the Simcyp platform for CYP3A4 induction. *CPT Pharmacometrics Syst Pharmacol*.

Chene P. Inhibiting the p53–MDM2 interaction: an important target for cancer therapy. *Nat Rev Cancer* 3(2), 102–109 (2003)

Cleary Y, Gertz M, Morcos PN, Yu L, Youdim K, Phipps A, Fowler S, and Parrott N (2018) Model-Based Assessments of CYP-Mediated Drug-Drug Interaction Risk of Alectinib: Physiologically Based Pharmacokinetic Modeling Supported Clinical Development. *Clin Pharmacol Ther* **104:**505-514.

Ding Q, Zhang Z, Liu JJ et al. Discovery of RG7388, a potent and selective p53-MDM2 inhibitor in clinical development. *J Med Chem* 56(14), 5979–5983 (2013).

Emami Riedmaier A, Lindley DJ, Hall JA, Castleberry S, Slade RT, Stuart P, Carr RA, Borchardt TB, Bow DAJ, and Nijsen M (2018) Mechanistic Physiologically Based Pharmacokinetic Modeling of the Dissolution and Food Effect of a Biopharmaceutics Classification System IV Compound-The Venetoclax Story. *J Pharm Sci* **107:**495-502.

Fahmi OA, Maurer TS, Kish M, Cardenas E, Boldt S, and Nettleton D (2008) A combined model for predicting CYP3A4 clinical net drug-drug interaction based on CYP3A4 inhibition, inactivation, and induction determined in vitro. *Drug Metab Dispos* **36:**1698-1708.

Fahmi OA, Hurst S, Plowchalk D, Cook J, Guo F, Youdim K, Dickins M, Phipps A, Darekar A, Hyland R, and Obach RS (2009) Comparison of different algorithms for predicting clinical drug-drug interactions, based on the use of CYP3A4 in vitro data: predictions of compounds as precipitants of interaction. *Drug Metab Dispos* **37:**1658-1666.

Freise KJ, Shebley M, and Salem AH (2017) Quantitative Prediction of the Effect of CYP3A Inhibitors and Inducers on Venetoclax Pharmacokinetics Using a Physiologically Based Pharmacokinetic Model. *J Clin Pharmacol* **57:**796-804.

Glenn KJ, Yu LJ, Reddy MB, Fretland AJ, Parrott N, Hussain S, Palacios M, Vazvaei F, Zhi J, and Tuerck D (2016) Investigating the effect of autoinduction in cynomolgus monkeys of a novel anticancer MDM2 antagonist, idasanutlin, and relevance to humans. *Xenobiotica* **46:**667-676.

Haupt Y, Maya R, Kazaz A, Oren M. Mdm2 promotes the rapid degradation of p53. *Nature* 387(6630), 296–299 (1997)

Heimbach T, Chen Y, Chen J, Dixit V, Parrott N, Peters SA, Poggesi I, Sharma P, Snoeys J, Shebley M, Tai G, Tse S, Upreti VV, Wang YH, Tsai A, Xia B, Zheng M, Zhu AZX, and Hall S (2021) Physiologically-Based Pharmacokinetic Modeling in Renal and Hepatic Impairment Populations: A Pharmaceutical Industry Perspective. *Clin Pharmacol Ther* **110:**297-310.

Herting, Frank, et al. "Chemotherapy-free, triple combination of obinutuzumab, venetoclax and idasanutlin: antitumor activity in xenograft models of non-Hodgkin lymphoma." *Leukemia & lymphoma* 59.6 (2018): 1482-1485.

Higgins B, Tovar T, Glenn K et al. Antitumor activity of the MDM2 antagonist RG7388. *Mol Cancer Ther* 12(Suppl. 11) , Abstract B55 (2013).

Italiano A, Miller WH, Jr., Blay JY, Gietema JA, Bang YJ, Mileshkin LR, Hirte HW, Higgins B, Blotner S, Nichols GL, Chen LC, Petry C, Yang QJ, Schmitt C, Jamois C, and Siu LL (2021) Phase I study of daily and weekly regimens of the orally administered MDM2 antagonist idasanutlin in patients with advanced tumors. *Invest New Drugs*.

Jiang X, Zhuang Y, Xu Z, Wang W, and Zhou H (2016) Development of a Physiologically Based Pharmacokinetic Model to Predict Disease-Mediated Therapeutic Protein-Drug Interactions: Modulation of Multiple Cytochrome P450 Enzymes by Interleukin-6. *AAPS J* **18:**767-776.

Johnson TN, Tucker GT, Tanner MS, and Rostami-Hodjegan A (2005) Changes in liver volume from birth to adulthood: a meta-analysis. *Liver Transpl* **11:**1481-1493.

Kadia TM, Jain P, Ravandi F et al. TP53 mutations in newly diagnosed acute myeloid leukemia: clinicomolecular characteristics, response to therapy and outcomes. *Cancer* 122(22), 3484–3491 (2016).

Kubbutat MH, Jones SN, Vousden KH. Regulation of p53 stability by Mdm2. *Nature* 387(6630), 299–303 (1997).

Machavaram KK, Endo-Tsukude C, Terao K, Gill KL, Hatley OJ, Gardner I, Parrott N, and Ducray PS (2019) Simulating the Impact of Elevated Levels of Interleukin-6 on the Pharmacokinetics of Various CYP450 Substrates in Patients with Neuromyelitis Optica or Neuromyelitis Optica Spectrum Disorders in Different Ethnic Populations. *AAPS J* **21:**42.

Mascarenhas, John, et al. Oral idasanutlin in patients with polycythemia vera. Blood, *The Journal of the American Society of Hematology* 134.6 (2019): 525-533.

Melo MB, Ahmad NN, Lima CS et al. Mutations in the p53 gene in acute myeloid leukemia patients correlate with poor prognosis. *Hematology* 7(1), 13–19 (2002).

Moll UM, Petrenko O. The MDM2–p53 interaction. *Mol Cancer Res* 1(14), 1001–1008 (2003).

Nemunaitis J, Young A, Ejadi S, Miller W, Chen LC, Nichols G, Blotner S, Vazvaei F, Zhi J, and Razak A (2018) Effects of posaconazole (a strong CYP3A4 inhibitor), two new tablet formulations, and food on the pharmacokinetics of idasanutlin, an MDM2 antagonist, in patients with advanced solid tumors. *Cancer Chemother Pharmacol* **81:**529-537.

Njuguna NM, Umehara KI, Huth F, Schiller H, Chibale K, and Camenisch G (2016) Improvement of the chemical inhibition phenotyping assay by cross-reactivity correction. *Drug Metab Pers Ther* **31:**221-228.

Papai Z, Chen LC, Da Costa D, Blotner S, Vazvaei F, Gleave M, Jones R, and Zhi J (2019) A single-center, open-label study investigating the excretion balance, pharmacokinetics, metabolism, and absolute bioavailability of a single oral dose of [(14)C]-labeled idasanutlin and an intravenous tracer dose of [(13)C]-labeled idasanutlin in a single cohort of patients with solid tumors. *Cancer Chemother Pharmacol* **84:**93-103.

Park JY, Kim KA, Kang MH, Kim SL, and Shin JG (2004) Effect of rifampin on the pharmacokinetics of rosiglitazone in healthy subjects. *Clin Pharmacol Ther* **75:**157-162.

Vasilogianni AM, Al-Majdoub ZM, Achour B, Peters SA, Rostami-Hodjegan A, and Barber J (2021) Proteomics of Colorectal Cancer Liver Metastasis: a Quantitative Focus on Drug Elimination and Pharmacodynamics Effects. *Br J Clin Pharmacol*.

Vyhlidal CA, Chapron BD, Ahmed A, Singh V, Casini R, and Shakhnovich V (2021) Effect of Crohn's Disease on Villous Length and CYP3A4 Expression in the Pediatric Small Intestine. *Clin Transl Sci* **14:**729-736.

Xu Y, Hijazi Y, Wolf A, Wu B, Sun YN, and Zhu M (2015) Physiologically Based Pharmacokinetic Model to Assess the Influence of Blinatumomab-Mediated Cytokine Elevations on Cytochrome P450 Enzyme Activity. *CPT Pharmacometrics Syst Pharmacol* **4:**507-515.

Yee K, Papayannidis C, Vey N, Dickinson MJ, Kelly KR, Assouline S, Kasner M, Seiter K, Drummond MW, Yoon SS, Lee JH, Blotner S, Jukofsky L, Pierceall WE, Zhi J, Simon S, Higgins B, Nichols G, Monnet A, Muehlbauer S, Ott M, Chen LC, and Martinelli G (2021) Murine double minute 2 inhibition alone or with cytarabine in acute myeloid leukemia: Results from an idasanutlin phase 1/1b study small star, filled. *Leuk Res* **100:**106489.

Footnotes

a) This research was supported by Roche Pharmaceutical Research and Early Development.

b) No author has an actual or perceived conflict of interest with the contents of this article.

Reprint requests:

Kenichi Umehara, Ph.D.

Roche Pharmaceutical Research and Early Development

Grenzacherstrasse 124, CH-4070 Basel, Switzerland.

Tel.: +41-61-68-80821.

E-mail: kenichi.umehara@roche.com

Figure legends

Figure 1. A schematic description of disposition pathways of idasanutlin and RO6802287 (M4)

Derivation of the drug disposition pathways for idasanutlin and the major circulating metabolite M4 is described in Materials and Methods. F_a was calculated based on the absolute bioavailability study results. Contributions of CYP3A4 and CYP2C8 to total elimination of idasanutlin were estimated in alignment with the *in vitro* enzymology and the systemic exposure change of idasanutlin after co-administration of posaconazole. Sum of fractions eliminated by UGT1A3 and biliary excretion are based on the human mass balance study data. Disposition of M4 was derived from human mass balance data.

1) Two values in SDP and MBP formulation at fed state

2) A prediction using the current PBPK model in SimCYP Version 18

Figure 2. A summary workflow illustrating idasanutlin PBPK model building and application

The model building details for idasanutlin and RO6802287 (M4) are described in Materials and Methods. QWBA and MD represent quantitative whole body autography and multiple dosing, respectively.

Figure 3. Mean plasma concentration-time profiles of idasanutlin and M4

Plasma concentration time profiles of idasanutlin after intravenous administration of idasanutlin 0.1 mg (A) (observations: n=8; simulations: n=80), plasma concentration time profiles of idasanutlin (B) and M4 (C) after oral administration of idasanutlin 400

mg on Days 1, 10 and 19 over 30-day cycle (observations: n=28; simulations: n=100) are presented in semi-logarithmic scale. The 5th to 95th percentiles of the predictions (grey shaded areas), median (grey solid lines) and the observations (open circles) are shown.

Figure 4. Predicted and observed plasma concentration of idasanutlin in the absence and presence of posaconazole

Geometric means of the observed and predicted idasanutlin plasma concentrations in the absence (observations = open circles and predictions = dotted lines) and presence of posaconazole (observations = solid squares and predictions = solid lines) are compared. Simulations were repeated 10 times and each line indicates the geometric mean of each trial.

Figure 5. Forest plot to compare the DDI effects of CYP2C8 and CYP3A4 perpetrators at steady-state on single dose PK of idasanutlin after oral administration

Predicted AUC_{inf} ratio (closed diamond) and C_{max} ratio (open circle) of idasanutlin (300 or 400 mg p.o., single dose at day 5, 7 or 15) with co-medication of multiple oral administration of strong CYP3A4 inhibitors (itraconazole: 200 mg once daily, ketoconazole: 200 mg twice daily, posaconazole: 400 mg twice daily), moderate CYP3A4 inhibitors (erythromycin: 500 mg twice daily, fluconazole: 200 mg once daily), a weak CYP3A4 inhibitor (fluvoxamine: 50 mg once daily), a strong CYP2C8 inhibitor gemfibrozil (600 mg twice daily), a moderate CYP3A4(/2C8) inducer efavirenz (600 mg once daily) and a strong CYP3A4 and CYP2C8 inducer rifampicin (600 mg once

daily) are plotted. The dual inhibition effects of simultaneous administration of gemfibrozil and ketoconazole on CYP2C8 and CYP3A4 were also evaluated as a worst case inhibition scenario. The impact of rifampicin on CYP2C8 and CYP3A4 can be independently simulated in this study. The efavirenz model was not verified as a CYP2C8 inducer.

Simulated data represented geometric mean with 95% interval (n=100), except for the posaconazole DDI data (geometric mean with range, n=20 for observation and n=200 for verification). The ratios in green closed, green broken and red broken boxes are the reference values, the predicted values with the current idasanutlin model verified based on the clinical data, and the predicted values without the corresponding measured data, respectively.

DMD Fast Forward. Published on December 22, 2021 as DOI: 10.1124/dmd.121.000720
This article has not been copyedited and formatted. The final version may differ from this version.

Tables

Table 1. Outline of the simulation work

Substrate	Perpetrator	Pathway	Site where DDI occurs	Inhibited by the parent drug (static calculation)	Inhibited by M4 (static calculation)
Midazolam	Idasanutlin	CYP3A4	Liver (and intestine)	X	
Repaglinide		CYP2C8 CYP3A4	Liver (and intestine)	X	X
Idasanutlin	Posaconazole Ketoconazole Itraconazole	CYP3A4	Liver and intestine	Inhibition	
	Gemfibrozil	CYP2C8	Liver	Inhibition	
	Rifampicin	CYP3A4 CYP2C8	Liver and intestine	Induction	

DMD Fast Forward. Published on December 22, 2021 as DOI: 10.1124/dmd.121.000720
This article has not been copyedited and formatted. The final version may differ from this version.

Table 2. Parameter values used for PBPK modeling of idasanutlin and the major circulating metabolite M4 as a perpetrator and/or a victim drug on CYPs

Input parameters	Units	Idasanutlin (perpetrator and victim)		M4 (perpetrator)	
		Value	Remarks	Value	Remarks
1.Physicochemical and binding properties					
MW	g/mol	616.49		630.47	Calculated
Log P	-	5.6		4.97	Calculated
Compound type	-	Ampholyte		Ampholyte	Calculated
pKa	-	4 (acid) / 6.9 (base)		3.97 (acid) / 7.11 (base)	
B/P ratio	-	0.64		1	Assumption
fu	-	0.001	Measured as < 0.1%	0.001	Measured as < 0.1%
HSA or AGP	-	HSA		HSA	Assumption
2.Absorption					
Absorption model	First order absorption model [1]			-	
fa	-	0.401	[2]	-	-
CV fa	%	30	[3]	-	-
ka	1/h	0.35	[2]	-	-
CV ka	%	30	[3]	-	-
Peff,man	10^{-4} cm/s	0.525	Prediction [3]	-	-
P caco-2	10^{-6} cm/s	0.8		-	-
P propranolol	10^{-6} cm/s	14		-	-
fu(gut)	-	0.001	Assumption:=fu	1	[7]
Q(gut)	L/h	3.88	Prediction [3]	-	-
CV Q(gut)	%	30	[3]	-	-
3.Distribution					
Distribution model	Full PBPK model				
Tissue model	Perfusion limited model				
Vss	L/kg	0.40	[4]	0.426	[4]
CV Vss	%	30	[3]	30	[3]
4.Enzyme phenotyping					
Recombinant CYP enzymes					
CLint (CYP3A4)	µL/min/pmol	0.42	[5]	-	-
CLint (CYP2C8)	µL/min/pmol	2.5	[5]	-	-
5.Other Distribution and Elimination property					
In vivo CL					
CLr	L/h	0		0	[8]
CL	L/h	-	-	1.76	[9]
CV CL	%	-	-	30	[3]
In vitro CL					
HLM CLint (unbound)	µL/min/mg	110	[6]	-	-
CV HLM CLint	%	30	[3]	-	-
7.Interaction					
CYP inhibition (competitive)					
Ki (CYP2C8)	µM	0.082	= IC_{50}/2	0.065	= IC_{50}/2
fu(mic) (CYP2C8)	-	0.035		0.916	Prediction [10]

DMD Fast Forward. Published on December 22, 2021 as DOI: 10.1124/dmd.121.000720
This article has not been copyedited and formatted. The final version may differ from this version.

Input parameters	Units	Idasanutlin (perpetrator and victim)		M4 (perpetrator)	
		Value	Remarks	Value	Remarks
Ki (CYP3A4)	μM	25	= IC_{50}/2	4.6	= IC_{50}/2
fu(mic) (CYP3A4)	-	0.05		0.731	Prediction [10)]

1) No involvement of intestinal efflux transporters in the absorption process

2) For SDP formulation at fed state

3) SimCYP Version 18

4) The idasanutlin V_{ss} was initially predicted using the K_p values determined in rats, then scaling all of the K_p values by 50% delivered consistent V_{ss} and plasma concentration–time profiles after i.v. administration of [^{13}C]-idasanutlin. The K_p values were 0.352 (lung), 0.384 (adipose), 0.800 (pancreas), 0.320 (muscle), 3.01 (liver), 0.545 (spleen), 0.705 (heart), 0.128 (brain), 1.135 (kidney), 0.256 (skin), 0.448 (bone marrow) and 1.135 (gut). The K_p values of M4 was assumed to be identical with the parent drug.

5) In vivo fm,CYP3A4 and F_g were estimated from the clinical DDI study with posaconazole by two-dimensional analyses (Cleary et al. 2018). fmCYP2C8 was estimated according to the in vitro enzymology data and the estimated in vivo fm,CYP3A. CYP3A4 and CYP2C8 catalyzed the formation of M2 and M2 was further metabolized to M4. Therefore, the assigned intrinsic clearance due to CYP3A4 and CYP2C8 was regarded as the M4 formation clearance.

6) The CLint was back-calculated by assuming that it represents the combined contributions of UGT1A3 and (potential) biliary excretion to total elimination based on the in vitro enzymology and human mass balance study results

7) A worst case scenario for the perpetrator DDI liability assessment

8) Negligible amount of the radioactivity derived from M4 was observed in urine from the human mass balance study results of idasanutlin

9) Adapted to capture the observed plasma concentration profiles over time for M4 after the last dose of idasanutlin at 400 mg p.o. on days 1, 10 and 19

10) Based on a concentration of human liver microsomes at 0.0125 mg/mL in the in vitro assay

Table 3. Predictions of the exposure changes for midazolam and repaglinide when combined with repeated oral doses of idasanutlin

Victim	Day X	Model	Perpetrator	N	C_{max} (ng/mL)	AUC_{inf} (ng·h/mL)	C_{max} ratio	AUC ratio
Midazolam (2 mg p.o., single dose) at day X after administration of the perpetrator	5	Idasanutlin +M4	Alone	100	9.70 (CV: 54%)	25.7 (CV: 74%)	-	-
			+Idasanutlin (300 mg p.o., twice daily for 5 days)		11.6 (CV: 52%)	30.9 (CV: 70%)	1.19 (CV: 10%)	1.20 (CV: 10%)
Repaglinide (0.25 mg p.o., single dose) at day X after administration of the perpetrator	5	Idasanutlin only	Alone	100	3.82 (CV: 46%)	5.04 (CV: 75%)	-	-
			+Idasanutlin (300 mg p.o., twice daily for 5 days)		5.02 (CV: 17%)	8.10 (CV: 76%)	1.31 (CV: 11%)	1.61 (CV: 17%)
	5	Idasanutlin +M4	Alone	100	3.82 (CV: 46%)	5.04 (CV: 75%)	-	-
			+Idasanutlin (300 mg p.o., twice daily for 5 days)		5.66 (CV: 40%)	9.89 (CV: 74%)	1.48 (CV: 16%)	1.96 (CV: 24%)

Pharmacokinetic data are presented as geometric mean with CV(%) in parentheses.

Table 4. Summary of PK parameters in the absence and presence of posaconazole

Parameters	Idasanutlin (800 mg p.o., single dose) alone		Idasanutlin and posaconazole (400 mg p.o., twice daily)	
	Observation (Nemunaitis, et al., 2018)	Prediction	Observation (Nemunaitis, et al., 2018)	Prediction
n	20	200	20	200
T_{max} (hr)	9.53 [5.95 – 50.5]	9.83 [4.75 – 20.6]	9.52 [5.92 – 24.7]	10.7 [5.5 – 21.7]
C_{max} (ng/mL)	3950 (40.0%)	4300 (21.0%)	3700 (56.2%)	4520 (20.0%)
AUC_{inf} (ng•h/mL)	217,000 (34.0%)	213,000 (46%)	283,000 (43.5%)	273,000 (45.0%)
$t_{1/2}$ (hr)	34.6 (35.0%)	25.5 (43.0%)	41.6 (76.7%)	26.1 (43.0%)
C_{max} ratio	-	-	0.935 [0.782-1.12]	1.05 [1.05-1.05]
AUC_{inf} ratio	-	-	1.31 [1.08-1.58]	1.28 [1.26 – 1.30]

Geometric mean (CV%) is presented for all parameters except for T_{max} where median and range are shown.

Table 5. Predictions of the idasanutlin exposure changes on Day 5 after repeated idasanutlin doses when combined with repeated perpetrators on CYP3A4 and CYP2C8 inhibitors/inducers

Victim	Day X	Model	Inhibition	CYP enzyme inhibited/induced	N	C_{max} (ng/mL)	$AUC_{(0-t)}$ (ng·h/mL)	C_{max} ratio	AUC ratio
Idasanutlin, multiple dose (300 mg p.o., twice daily for the last 5 days) at Day X after the last dose	30 [1)]	Idasanutlin	Without inhibitor	-	100	12519 (3711-45065)	254993 (64960-1031275)	-	-
			+ itraconazole (200 mg p.o., once daily, 30 days)	CYP3A4	100	14630 (3968-50399)	307257 (71645-1168758)	1.17 (1.07-1.33)	1.21 (1.08-1.42)
	15		Without inhibitor	-	100	12688 (3749-39552)	144927 (40905-466170)	-	-
			+ gemfibrozil (600 mg p.o., twice daily, 15 days)	CYP2C8	100	15494 (5694-40778)	179203 (61558-481062)	1.22 (1.02-2.00)	1.24 (1.03-2.11)
	15		Without inhibitor	-	100	12973 (3628-41142)	148473 (39437-481730)	-	-
			+ ketoconazole (200 mg p.o., twice daily, 15 days) + gemfibrozil (600 mg p.o., twice daily, 15 days)	CYP3A4 CYP2C8	100	20321 (7820-56033)	238124 (87341-1662719)	1.57 (1.11-2.43)	1.60 (1.11-2.63)
	15 [1)]		Without inducer	-	100	12514 (4094-43958)	254951 (74486-1002730)	-	-
			+ rifampicin (600 mg p.o., once daily, 15 days)	CYP3A4 CYP2C8	100	4360 (1201-18033)	62213 (12199-347648)	0.35 (0.25-0.50)	0.24 (0.15-0.45)

Pharmacokinetic data are presented as geometric mean with range in parentheses.

1) The 2nd dose at the last treatment day 15 was not administered in the simulation design.

Figure 1

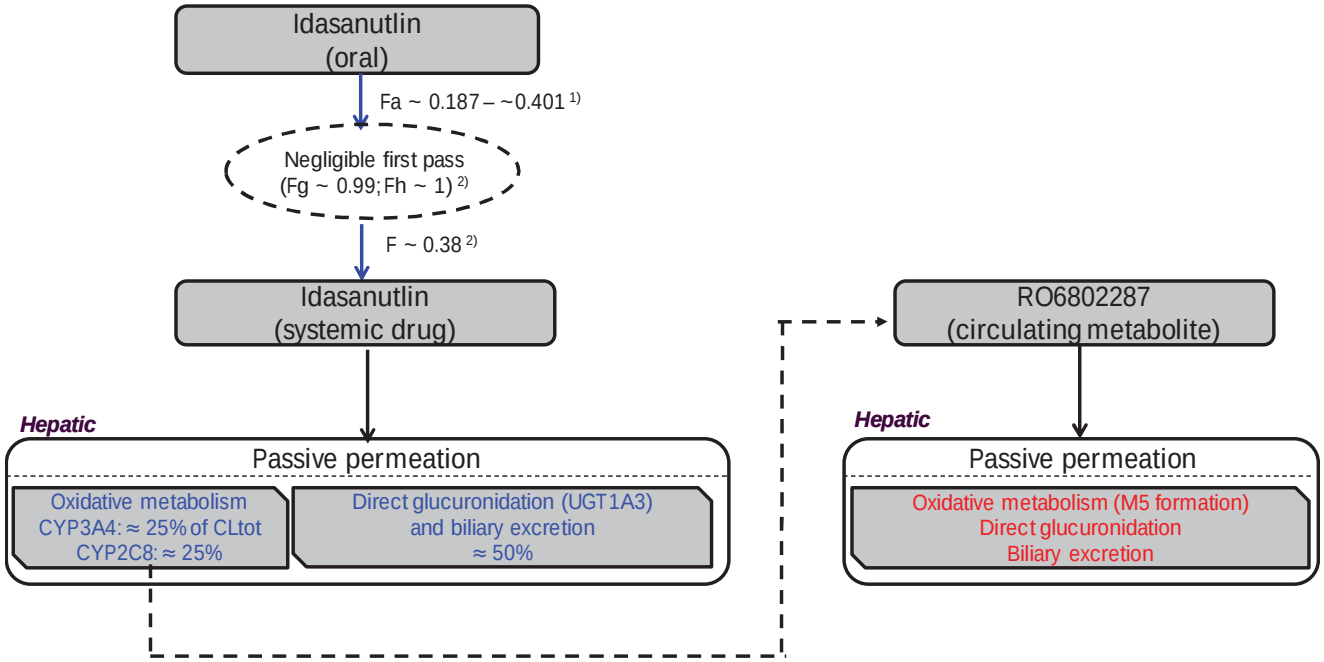

Figure 2

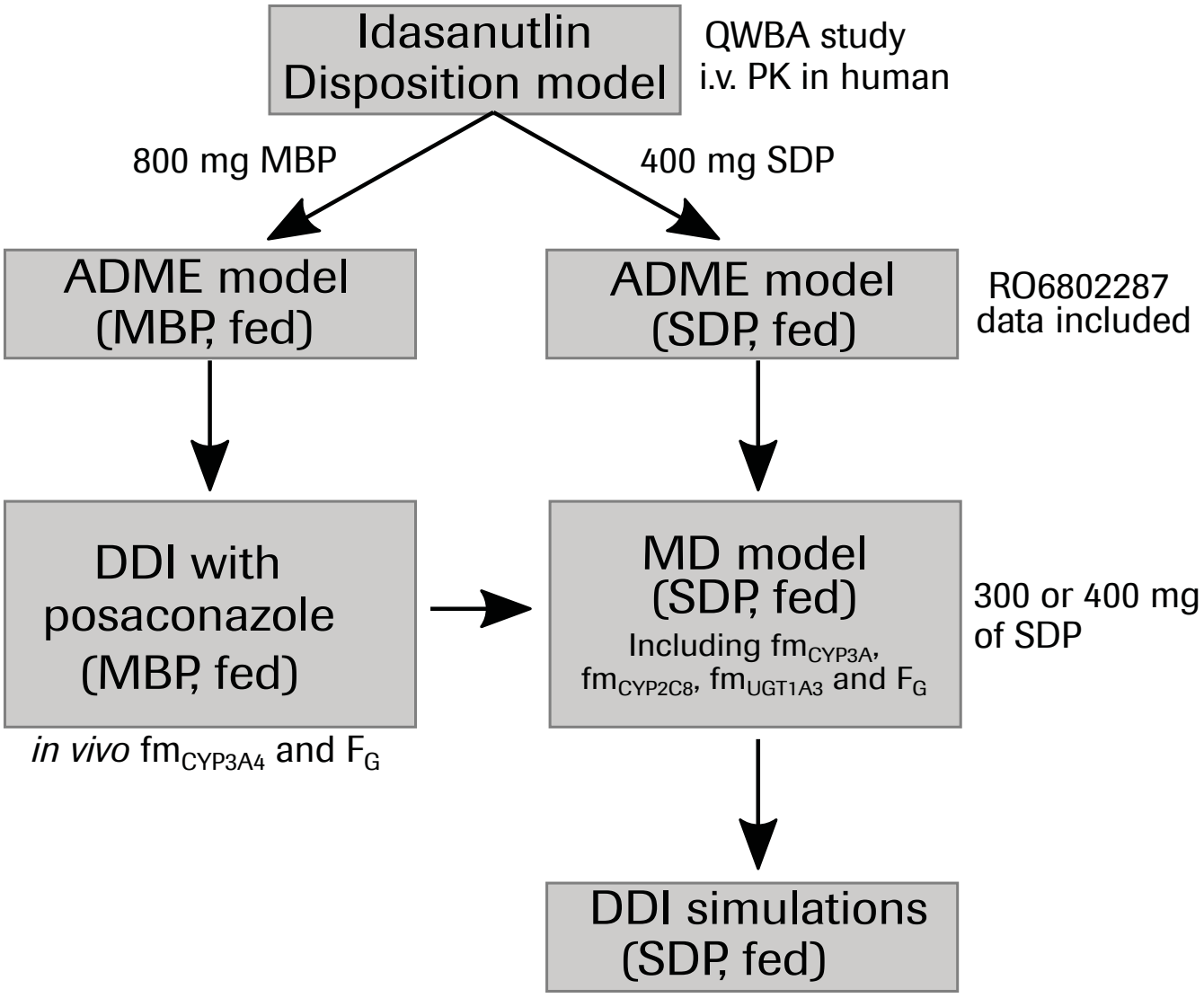

Figure 3

DDI-PBPK modeling of idasanutlin

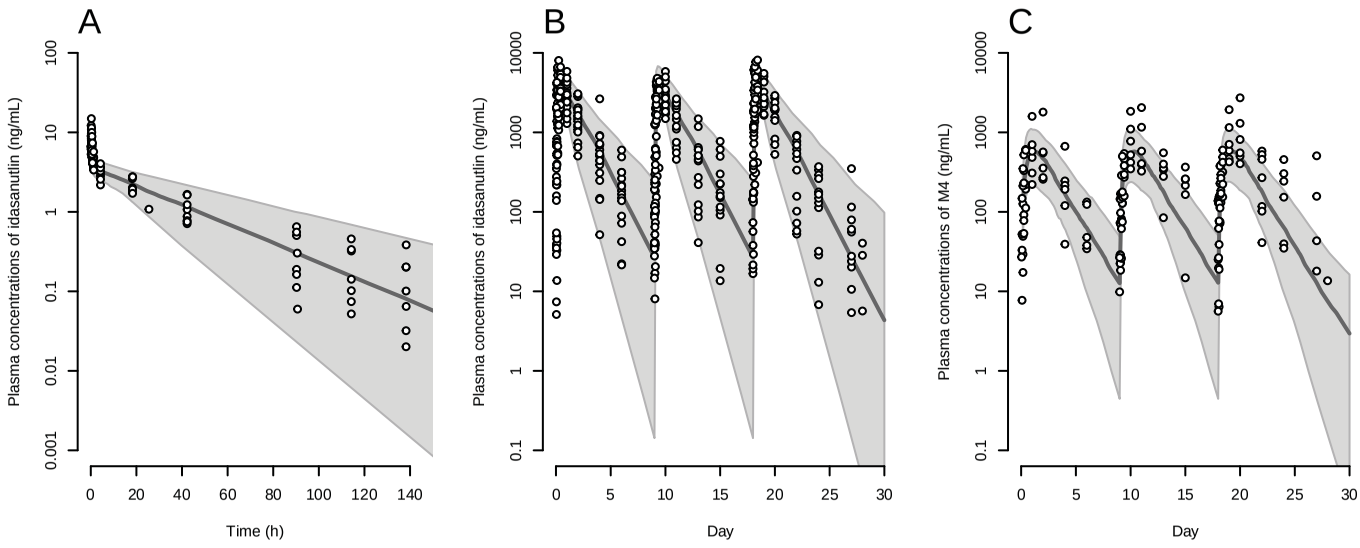

Figure 4

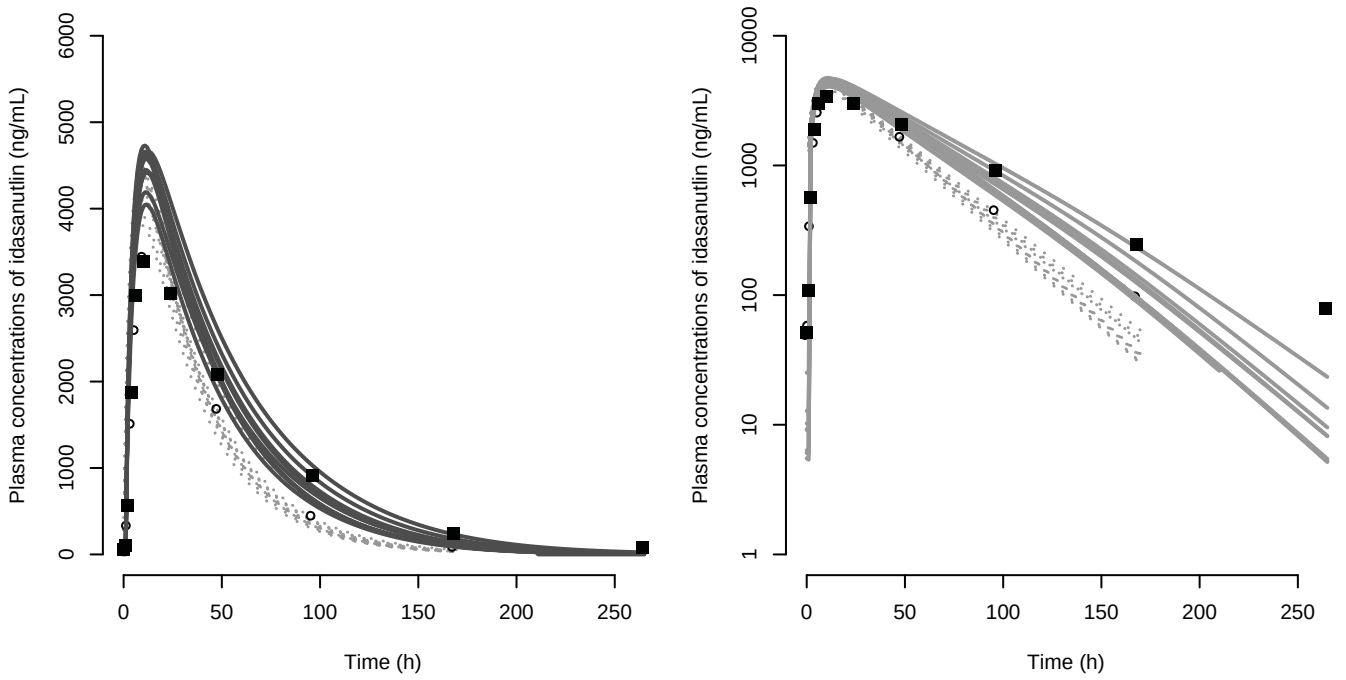

Figure 5